Mode matching with a phase camera for gravitational-wave detectors

Ricardo Cabrita[a,*], Clément Lauzin[a], Giacomo Bruno[a], Joris van Heijningen[a,b]

[a] *Universite Catholque de Louvain, 2, Chemin du Cyclotron, 1348, Louvain-la-Neuve, Belgium*
[b] *Vrjie Universiteit Amsterdam, Address, Postcode, Amsterdam, Netherlands*

Abstract

Mode mismatch causes a large fraction of optical losses in gravitational-wave detectors. This effect will need to be considerably reduced in next generation detectors in order to fully exploit advanced techniques such as squeezing. Phase cameras are wavefront sensors capable of imaging the amplitude and phase of a laser beam. We simulate a measurement scheme with the phase camera and show that the two resulting error signals can be used to act on the two mismatch degrees of freedom in a closed loop.

Keywords: Gravitational-wave detectors, mode matching, wavefront sensing, optics

1. Introduction

Currently, mode mismatch accounts for a large fraction of optical losses in gravitational-wave (GW) detectors [1]. Optical losses are one of the greatest obstacle towards achieving the quantum noise reduction goals of next-generation detectors [2]. Furthermore, next-generation detectors plan to increase the circulating power up to 3 MW [3]. At such high powers, absorption leads to thermal lenses and changes to the radius of curvature in mirrors and other optics, shifting the optimal mode matching conditions. For this reason, active sensing and compensation of mode mismatch is needed for future GW detectors. While multiple schemes have already been proposed, very few implementations are currently in use [1] and none in a closed loop.

Building on previous work [4], we show how a phase camera monitoring the reflected beam from a cavity can generate mode matching error signals to be used in a closed loop and how they couple to the two mismatch quadratures.

2. Phase camera and linear cavity mode matching

In GW detectors it is common for the circulating beam to have a carrier and multiple sideband spectral components, which are used to keep the various cavities in resonance [5]. The phase camera considered in this work is shown in fig. 1. It is able to image each carrier and sideband separately, by interfering the beam with a frequency-shifted reference beam. A fast photodiode with enough bandwidth is necessary to acquire the signal. The beam is scanned over the pinhole of the photodiode and the image is reconstructed. For each each pixel and frequency the signal is demodulated into I/Q quadratures, from which the amplitude and phase is retrieved. [6].

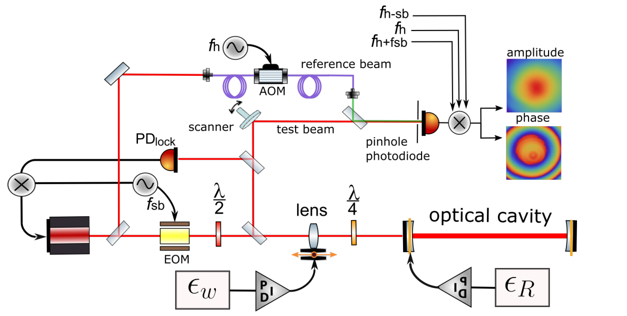

Figure 1: Optical set-up modelled in this work, with a phase camera [6] monitoring the reflection from a cavity. The error signals detailed in the text could be used to act on a lens position and a ring heater on the cavity input mirror [1].

For what concerns optical cavities, mode mismatch refers to a mismatch between the shape of the input beam and the eigenmode of a cavity. Both the input beam and cavity modes can be parameterised by their respective beam parameters, a complex number of the form $q = z + z_R$ [7], where z is the distance to the waist of the beam, and $z_R = \pi w_0^2/\lambda$ is the Rayleigh range associated with a waist size w_0 and wavelength λ.

Optimal mode matching can be achieved either by acting on the cavity eigenmode parameter q_1, or the input beam parameter, q_2. An error signal should account for the difference between complex paramters q_1 and q_2. In [8], such a quantity is defined as

$$\epsilon_q = \frac{q_2 - q_1}{z_{R,1}} = \frac{\Delta z}{z_{R,1}} + i\frac{\Delta z_R}{z_{R,1}} = \epsilon_z + i\epsilon_{z_R}, \tag{1}$$

where ϵ_z and ϵ_{z_R} refer to waist position and waist size mismatch respectively. Current sensing schemes require two sensors to measure each mismatch quadrature independently [1].

3. Error signals with a single phase camera

The phase camera images the amplitude and phase of the beam in the x,y plane. From the amplitude we have access to the

*Corresponding author
Email address: `ricardo.cabrita@uclouvain.be` (Ricardo Cabrita)

beam radius, w, and from the phase to the radius of curvature, R. These quantities are related to q, via [7]

$$\frac{1}{q} = \frac{1}{R} - i\frac{\lambda}{\pi w^2}. \tag{2}$$

We can alternatively define the mode mismatch in the q reciprocal space, where optimal mode matching is achieved when $1/q_2 - 1/q_1 = 0$. This value, which we call ϵ'_q, is given by

$$\epsilon'_q = -\frac{\Delta R}{R_2 R_1} + i\frac{\lambda}{\pi}\frac{\Delta w^2}{w_2^2 w_1^2} = -\epsilon_R + i\epsilon_W, \tag{3}$$

with $\Delta R = R_2 - R_1$ and $\Delta w^2 = w_2^2 - w_1^2$. In fig. 2 we compare ϵ_R and ϵ_w with ϵ_Z and ϵ_{z_R}. As expected, both ϵ_R and ϵ_w couple to both mismatch quadratures. However, ϵ_R couples more closely to waist size mismatch while ϵ_w to waist position mismatch.

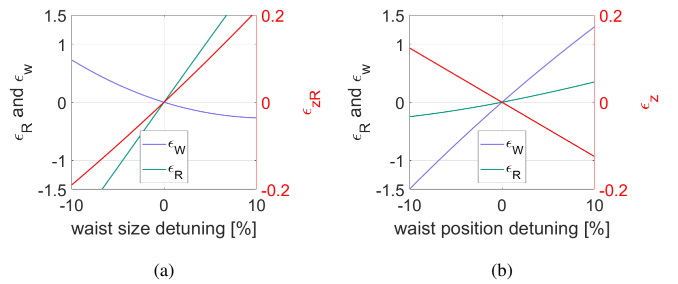

Figure 2: Computation of ϵ_R and ϵ_W from eq. 3 by detuning a) waist size and b) waist position relative to a $q_1 = 0.0426 + i0.0343$.

3.1. *Error signals proportional to ϵ_R and ϵ_w*

Optical simulation of the set-up presented in fig. 1 were done in OSCAR [9]. The same q used in fig. 2 is used for the input beam. The cavity is composed of two (fused silica) plano-concave mirrors with 0.1 m radius of curvature and a separation of 0.075 m in air. The cavity is overcoupled with a finesse of ≈ 800. These parameters are such that the set-up can be reproduced in a table-top experiment for validation. The reflected beam from the cavity is monitored just before the input mirror.

While the carrier is kept resonant with the cavity, the sidebands are non-resonant and have the same spatial mode as the input beam. Part of the reflected carrier field shares the mode of the cavity from the leakage field. The rest is from prompt reflection, mainly the second-order mode from mode mismatch. We validate through the simulations that if higher-order modes from misalignment are negligible and the total reflected field is approximately Gaussian, the error signals can be retrieved by comparing the carrier with the sidebands.

The error signal proportional to ϵ_R, $\mathrm{err_R}$, is extracted by subtracting the phase image of the carrier from one of the sidebands. In the presence of mode mismatch, the cross section of the differential phase is curved. The ΔR could be fitted from this cross section, but alternatively we can simply take the signed amplitude of the differential phase cross section.

In fig 3a we plot the resulting $\mathrm{err_R}$ while detuning the waist size of the input beam in the simulation. We also check the cross coupling of $\mathrm{err_R}$ with respect to the other quadrature. The presence of position mismatch causes a small offset in the zero-crossing of the error signal.

The error signal proportional to ϵ_w, $\mathrm{err_w}$, is obtained by subtracting the fitted radius of the carrier from the fitted radius of one of the sidebands.

In fig. 3b we plot the resulting $\mathrm{err_W}$ while detuning the waist position of the input beam in the simulation. We also check the cross coupling of $\mathrm{err_W}$ with respect to the other quadrature. As expected from fig. 2, the offsets are larger in this case.

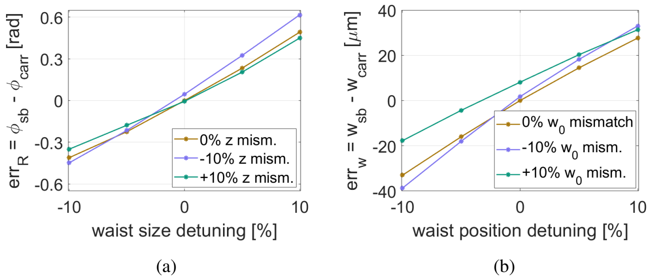

Figure 3: Simulated phase camera error signals (a) $\mathrm{err_R}$ vs. waist size, (b) $\mathrm{err_W}$ vs. waist position, and the impact of coupling to the opposing quadrature.

The offsets are well within the considered actuation range. Thus, the signals can be used in two feedback loops, one for each mismatch quadrature, converging to zero mode mismatch.

Finally, both error signals can be extracted separately for the x and y axis, making this scheme also sensitive to astigmatism.

4. Conclusion

We have shown how a single phase camera in a heterodyne scheme can generate error signals for automatic mode matching and how these signals couple to the waist size and position degrees of freedom. This highlights the potential of this kind of wavefront sensor for mode matching in next generation GW detectors.

References

[1] A. W. Goodwin-Jones, R. Cabrita, et al., Transverse mode control in quantum enhanced interferometers: a review and recommendations for a new generation, Optica 11 (2024) 273–290.
[2] P. Kwee, J. Miller, et al., Decoherence and degradation of squeezed states in quantum filter cavities, Phys. Rev. D 90 (2014) 062006.
[3] ET Steering Committee, Design Report Update 2020, ET-0007C-20 (2020).
[4] R. Cabrita, Sensing mode mismatch with the phase cameras at advanced virgo, Proceedings of GRASS2022 (2022).
[5] R. Drever, J. Hall, et al., Laser phase and frequency stabilization using an optical resonator, Applied Physics B 31 (1983) 97–105.
[6] K. Agatsuma, L. van der Schaaf, et al., High-performance phase camera as a frequency selective laser wavefront sensor for gravitational wave detectors, Opt. Express 27 (2019) 18533–18548.
[7] H. Kogelnik, T. Li, Laser beams and resonators, Applied Optics 5 (1966) 1550–1567.
[8] A. A. Ciobanu, D. D. Brown, et al., Mode matching error signals using radio-frequency beam shape modulation, Applied Optics 59 (2020) 9884.
[9] J. Degallaix, OSCAR: A MATLAB based package to simulate realistic optical cavities, SoftwareX 12 (2020) 100587.